

Decreased structural connectivity and resting-state brain activity in the lateral occipital cortex is associated with social communication deficits in boys with autism spectrum disorder

Minyoung Jung^{a,b}, Yiheng Tu^a, Courtney Amanda Lang^a, Ana Ortiz^a, Joel Park^a, Kristen Jorgenson^a, Xue-Jun Kong^c, Jian Kong^{a,*}

^a Department of Psychiatry, Massachusetts General Hospital, Harvard Medical School, Charlestown, MA, USA

^b Research Center for Child Mental Development, University of Fukui, Eiheiji, Fukui, Japan

^c Department of Internal Medicine, Beth Israel Deaconess Medical Center, Harvard Medical School, Lexington, MA, USA

ARTICLE INFO

Keywords:

Autism
Lateral occipital cortex
DTI
Resting-state fMRI
Surface area
fALFF

ABSTRACT

Autism spectrum disorder (ASD) is a prevalent neurodevelopmental disorder characterized by atypical social communication and repetitive behaviors. In this study, we applied a multimodal approach to investigate brain structural connectivity, resting state activity, and surface area, as well as their associations with the core symptoms of ASD. Data from forty boys with ASD (mean age, 11.5 years; age range, 5.5–19.5) and forty boys with typical development (TD) (mean age, 12.3; age range, 5.8–19.7) were extracted from the Autism Brain Imaging Data Exchange II (ABIDE II) for data analysis. We found significantly decreased structural connectivity, resting state brain activity, and surface area at the occipital cortex in boys with ASD compared to boys with TD. In addition, we found that resting state brain activity and surface area in the lateral occipital cortex was negatively correlated with communication scores in boys with ASD. Our results suggest that decreased structural connectivity and resting-state brain activity in the occipital cortex may impair the integration of verbal and non-verbal communication cues in boys with ASD, thereby impacting their social development.

1. Introduction

Autism spectrum disorder (ASD) is a neurodevelopmental disorder characterized by verbal and non-verbal communication deficits and repetitive behaviors (Lai et al., 2014). Despite the high prevalence of ASD, our understanding of the neurobiological mechanisms underlying the core symptoms of ASD is limited. Recently, multiple brain imaging tools have been used to explore the mechanisms of autism and have found that ASD is associated with atypical brain anatomical connectivity, gray matter volume, and resting-state functional activity / connectivity (Aoki et al., 2013; Bos et al., 2015; Di Martino et al., 2014; Schaer et al., 2013; Travers et al., 2012). Literature also suggests that these different brain imaging tools may investigate distinct aspects of brain structure and function.

Diffusion tensor imaging (DTI) is a widely applied brain imaging method used to investigate brain structural connectivity based on the strength of water diffusion and degree of anisotropy. DTI studies have shown that ASD is associated with disrupted white matter pathways,

including the superior longitudinal fasciculus, cingulum-cingulate gyrus supracallosal bundle (CCG), forceps major of the corpus callosum (FMAJ), forceps minor of the corpus callosum (FMIN), and uncinate fasciculus (UNC) (Alexander et al., 2007; Aoki et al., 2013; Barnea-Goraly et al., 2004; Brito et al., 2009; Kumar et al., 2010; Travers et al., 2012). In addition, altered structural connectivity has been found to be correlated with core symptoms of ASD (Aoki et al., 2013; Travers et al., 2012). These findings suggest there may be significant microstructural abnormalities and alterations in the organization of white matter (WM) fibers in ASD, which may impair normal brain functions.

Resting state fMRI is another widely used imaging method that investigates the brain mechanisms of ASD. There are many resting state fMRI data analysis methods, some of which focus on long-range connectivity among different brain regions, such as seed-based resting state functional connectivity (Di Martino et al., 2013; Jung et al., 2014) and independent component analysis (Uddin et al., 2013; von dem Hagen et al., 2013), and others which, focus on local connectivity and examine the properties of spontaneous local brain activity, such as fractional

* Corresponding author. Department of Psychiatry, Massachusetts General Hospital, Harvard Medical School, Charlestown, MA 02129, USA.

E-mail address: kongj@nmr.mgh.harvard.edu (J. Kong).

Abbreviations

ABIDE II	Autism brain imaging data exchange II	FMAJ	Forceps major of the corpus callosum
ADI-R	Autism diagnostic interview–revised	FMIN	Forceps minor of the corpus callosum
ASD	Autism spectrum disorder	ILF	Inferior longitudinal fasciculus
ATR	Anterior thalamic radiation	MD	Mean diffusivity
BET	Brain extraction tool	SCQ	Social communication questionnaire
CCG	Cingulum-cingulate gyrus supracallosal bundle	SRS	Social responsiveness scale
CSF	Cerebrospinal fluid	TBSS	Tract-based spatial statistics
DTI	Diffusion tensor imaging	TD	Typical development
fALFF	Low-frequency fluctuations	TOI	Tracts of interest
FA	Fractional anisotropy	TRACULA	Tracts constrained by underlying anatomy
		UNC	Uncinate fasciculus
		VBM	Voxel-based morphometry

amplitude of low-frequency fluctuations (fALFF) (Di Martino et al., 2014; Itahashi et al., 2015). One characteristic of local connectivity methods such as fALFF is that unlike distant connectivity methods that explore the association between different brain regions / networks, local connectivity methods can help target key regions involved in ASD. For instance, a previous study has shown that individuals with ASD have abnormal fALFF at the dorsal lateral prefrontal cortex, insula, posterior medial prefrontal cortex and occipital cortex compared to typical development (TD) individuals (Di Martino et al., 2014), highlighting the involvement of these regions in the pathology of ASD.

Recently, surface area analysis has also drawn the attention of autism researchers. This method has the potential to provide information about the intrinsic topology of the cerebral cortex and allow us to better understand the neurobiological mechanisms associated with brain alterations in ASD (Ecker et al., 2015). For example, abnormal surface area has been observed in the orbitofrontal and lateral occipital regions in individuals with ASD (Ecker et al., 2015; Wallace et al., 2013), suggesting the involvement of these regions in ASD.

Thus, neuroimaging evidence coming from DTI, fALFF, and structural MRI will provide information about different aspects of brain structure and function (i.e., white matter, local connectivity, and intrinsic topology of the cerebral cortex). The combination of these methods in the same cohort of participants will provide a more complete picture of the neuropathology of autism, which will significantly enhance our understanding of the mechanism underlying autism.

Nevertheless, only a few studies have combined multiple imaging modalities to explore brain anatomy, function, and connectivity simultaneously (Ecker et al., 2015; Libero et al., 2015). In a previous study, Libero and colleagues (Libero et al., 2015) found that combining multiple imaging modalities (structural MRI, DTI, 1H-MRS) may produce a high classification rate (91.9%) when distinguishing between adults with ASD and adults with TD. These findings have demonstrated the potential of multiple imaging modalities in autism research.

In this study, we applied DTI, resting state fMRI, and structural MRI to explore brain structural and functional changes in ASD, as well as the association between these changes and clinical outcomes using data from Autism Brain Imaging Data Exchange II (ABIDE II; http://fcon_1000.projects.nitrc.org/indi/abide/), a recently launched DTI and resting-state fMRI database. We hypothesized that individuals with ASD would show reduced anatomical connectivity and resting state brain activity compared to TD individuals. In addition, we predicted that these altered brain functional and structural changes in ASD individuals would be associated with ASD symptoms.

2. Materials and methods

2.1. Datasets

Data were extracted from Autism Brain Imaging Data Exchange II. Among the four institutions which collected DTI data, we used

datasets from the two (New York University = NYU and Trinity Center for Health Sciences = TCD) that collected the DTI data in a 3 T MRI scanner (Friedman et al., 2008), and focused on subjects between 6 and 19 years old to minimize potential developmental effects (Dickstein et al., 2013). All subjects from the two institutions were included in the data analysis if they met the following criteria: i) male (Baron-Cohen et al., 2005, 2003), ii) full scale IQ (F-IQ) scores >80 (Dichter and Belger, 2007), iii) diagnosis of ASD based on DSM-IV-TR, and assessed with the Autism Diagnostic Observation Schedule (Lord et al., 2000) or the Autism Diagnostic Interview–Revised (ADI-R) (Lord et al., 1994), or both. Individuals completed both the Social Responsiveness Scale (SRS), a 65-item rating measure that quantifies severity of ASD (Constantino et al., 2003) and the Social Communication Questionnaire (SCQ), a validated, parent-report screening measure that assesses the life-time severity of autism spectrum symptoms (Chandler et al., 2007).

2.2. Image data acquisition

DTI, resting-state fMRI scans, and anatomical scans were acquired on Siemens Allegra (Siemens Healthcare GmbH, Erlangen, Germany; NYU) and Philips 3 T Achieva (Philips Healthcare, Best, The Netherlands; TCD) MRI scanners. All subjects were asked to relax with their eyes open in the scanner. Site-specific protocols are detailed in [Supplemental Table S1](#).

2.3. DTI data analysis

To detect and correct any artifacts introduced during the collection of the DTI scan, we first computed the translation, rotation, portion of slices, signal drop-out score over all slice base on the diffusion weighted images (Yendiki et al., 2014), and any DTI volumes containing one or more artifacts were excluded. Finally, DTI images were corrected for head motion and eddy current artifacts using FSL (www.fmrib.ox.ac.uk/fsl/) tools. To define the tracts of interest (TOI), we performed voxel-wise analysis with tract-based spatial statistics (TBSS) (Smith et al., 2006). The voxels of the white matter skeleton ($FA > 0.2$) were registered to the FMRIB58_FA standard space template, the brain was extracted from beta images using the Brain Extraction Tool (BET), and the diffusion tensor model was fit using ddtfit in FSL (Smith et al., 2004). To specify structural connectivity in the human brain, we investigated fractional anisotropy (FA) and track length of white-matter pathways for each subject's native DTI using FreeSurfer's TRActs Constrained by UnderLying Anatomy (TRACULA) package, an automated probabilistic reconstruction package (Yendiki et al., 2011). FA and track length for each subject were standardized into z-scores by site, in order to reduce site-specific DTI parameter differences (White et al., 2011).

A two-sample *t*-test was applied to compare FA and track length differences between the two groups. The MRI site, FIQ, and age were also

included in the model as covariates. For the whole-brain analyses using TBSS, FSL's Randomize tool with threshold free cluster-enhancement (Smith and Nichols, 2009) was used to perform 10000 permutation tests with a significance threshold of $p < 0.05$ FWE corrected for multiple comparisons across voxels (Walker et al., 2012).

2.4. Resting-state fMRI data preprocessing

Resting-state fMRI datasets were preprocessed with SPM12 software (Wellcome Department of Cognitive Neurology, London, UK) and the CONN functional connectivity toolbox (<http://www.nitrc.org/projects/conn>) (Whitfield-Gabrieli and Nieto-Castanon, 2012). Resting-state data were realigned to the mean image and then volumes with a mean intensity $>1.5\%$ of the mean global signal or 0.5 mm/TR framework displacement were detected and removed using the ArtRepair toolbox to reduce the effect of head movement after deleting the first 10 vol (Bernard et al., 2016; Mazaika et al., 2009; Myers et al., 2016; Redcay et al., 2013; Wang et al., 2016). We performed CompCor correction and regressed out 6 motion parameters to reduce physiological and other noise artifacts (Muschelli et al., 2014). In addition, to investigate the effect of head motion and motion artifacts in resting state, mean frame-to-frame motion and frame-wise displacement were calculated for each participant. There were no significant differences in mean frame-to-frame motion ($p > 0.1$). We also included frame-wise displacement as a confounding factor in the group analysis, because there was a difference between the TD and ASD groups (p value is 0.042).

The fALFF calculation was performed using the REST toolbox (<http://resting-fmri.sourceforge.net>). Temporal band-pass filtering of the functional images (0.01–0.08 Hz) was used to remove low-frequency drift and high-frequency noise. The time series for each voxel was transformed to a frequency domain. The square root was calculated at each frequency of the power spectrum, and the sum of the amplitude across 0.01–0.08 Hz was divided by the square root across the entire frequency range.

To explore the between-group differences of fALFF patterns, two-sample t tests were performed on the z-transformed fALFF maps between ASD and TD groups using Gaussian random field theory. Four nuisance regressors (site, FIQ, frame displacement and age) were also included in the model. Finally, we conducted regression analyses between different measures (fALFF, surface area, tensor-based measures of track of interests using FA and track length) and core ASD symptom severity (ADI-R, SCQ and total SRS scores), adjusting for data collection site, FIQ, and age using SPSS. A threshold of $Z > 2.3$ and $p < 0.05$ corrected was applied in data analysis.

2.5. Surface area analysis

Anatomical image preprocessing was performed using FreeSurfer, version 5.3.0 (<http://surfer.nmr.mgh.harvard.edu/>) (Fischl, 2012). To increase anatomical validation across individuals with ASD and TD, FreeSurfer was used for segmentation of subcortical structures and automatic tessellation of the cortical surface. Automated segmentation and parcellation results were reviewed for quality and corrected by staff individually, as described in previous studies (Fischl et al., 2004, 1999a, 1999b; Han et al., 2006). Gray matter surface parcellation of each individual was based on the Desikan–Killiany parcellation atlas (Desikan et al., 2006)

Between-group differences for whole-brain analysis were corrected for multiple comparisons with a Monte Carlo z-field simulation at $p < 0.05$ (two-tailed). Group level analysis was carried out with four nuisance regressors (site, FIQ and age). In addition, we also defined regions of interest (ROI) based on the results from DTI analysis. Specifically, we defined 15 surface area ROIs connected to the DTI tracks that showed significant differences between the TD and ASD groups (Supplementary Table 2). A threshold of FDR $p < 0.05$ was applied for direct comparisons of 15 ROIs.

3. Results

3.1. Demographic and clinical characteristics

Forty boys with ASD (mean age, 11.5 years; age range, 5.5–19.5) and forty boys with TD (mean age, 12.3; age range, 5.8–19.7) were selected based on our inclusion criteria. There were significant differences in SRS total scores ($p < 0.001$) and SCQ scores ($p < 0.001$) between the two groups. There were no significant differences in site variation ($p = 0.82$), IQ ($p = 0.13$), or age ($p = 0.42$) between the two groups. However, FIQ, and age were included in the all group analysis as covariates for minimizing developmental factors. Demographic and clinical characteristics for all individuals are presented in Table 1.

3.2. DTI track

Tract-based spatial statistics revealed that the ASD group showed decreased FA in the right inferior longitudinal fasciculus (ILF), bilateral anterior thalamic radiation (ATR), bilateral CCG, right UNC, FMAJ, and FMIN (Fig. 1A). There were no significant FA increases in the ASD group compared to the TD group.

Probabilistic reconstruction analysis in TRACULA revealed that the ASD group showed significantly decreased FA ($p = 0.004$) and track length ($p = 0.04$) in the left CCG and right UNC (FA, $p = 0.01$; track length, $p = 0.04$) (Fig. 1B). In addition, ASD individuals also showed a negative correlation between the CCG track length and SCQ total scores ($p = 0.021$; $r = -0.396$) (Fig. 3).

3.3. Resting state activation

The ASD group showed decreased fALFF in the right cuneus and lateral occipital cortex compared to the TD group (Fig. 2). There were no fALFF increases in the ASD group compared to the TD group.

Regression analysis showed that there was a negative correlation between fALFF in the right lateral occipital cortex and ADI-R verbal scores ($p = 0.027$; $r = -0.369$) (Fig. 3B).

3.4. Surface area and cortical thickness

Using whole-brain analysis, there were no significant differences in surface area above the threshold we set between the ASD and TD groups.

Using ROI analysis, we found significantly reduced surface area at the right pericalcarine cortex (FDR $p < 0.05$) and right cuneus cortex (FDR $p < 0.05$) in the ASD group compared to the TD group. There was no difference between the ASD group and TD group. Please see Supplementary Table 3 and Table 4 for more details.

Regression analysis revealed significant negative correlations between surface area in the right lateral occipital cortex and ADI-R non-verbal scores ($p = 0.007$; $r = -0.439$), ADI-R verbal scores ($p = 0.001$; $r = -0.522$), and SRS total scores ($p = 0.027$; $r = -0.362$) (Fig. 4) in ASD individuals. There was no significant relationship between age and group differences (p values were below 0.1).

4. Discussion

In this study, we found that individuals with ASD had significantly 1) decreased structural connectivity in the right UNC and left CCG and 2) decreased fALFF and surface area in the right lateral occipital cortex and cuneus cortex. Finally, we found that these decreases in structural connectivity, fALFF, and surface area were associated with core symptoms of ASD. Our results suggest that the right occipital cortex may play an important role in the neuropathology of autism. We speculate the functional and structural alternations in this region may impair the integration of visual information, resulting in atypical social communication in individuals with ASD.

Our finding of decreased structural connectivity in the right UNC in

Table 1
Demographic and clinical characteristics of the autism brain imaging data exchange (ABIDE).

Measure	ASD			TD			ASD-TD group difference	
	n	mean	range	n	mean	range	t value	p value
Age (years)	40	11.5 (4.1)	6–19	40	12.3 (4.3)	6–19	–0.81	0.42
FIQ	40	110.1 (14.1)	86–139	40	115.6 (13.1)	81–132	–1.52	0.13
Institution ratio	40	NYU = 21, TCD = 19			40	NYU = 21, TCD = 19		
ADL-R								
Social	39	17.8 (5.4)	5–28	0				
Verbal	39	14.7 (4.4)	8–23	0				
Non-verbal	39	7.3 (3.2)	2–14	0				
ADOS total score	40	9.85 (3.6)	3–16	0				
SRS total scores	40	76.8 (13.6)	42–107	39	43.7 (6.6)	34–59	13.6	< .0001
SCQ total score	39	17.4 (8.4)	0–31	39	2.6 (2.3)	0–8	10.6	< .0001

ADI-R = Autism Diagnostic Interview Revised; ADOS = Autism Diagnostic Observation Schedule; ASD = autism spectrum disorders; NYU = New York University; SCQ = Social Communication Questionnaire; SRS = Social Responsiveness Scale; SD = standard deviation; TCD = Trinity Center for Health Sciences; TD = typically developing.

individuals with ASD is consistent with results from previous studies in adults (Thomas et al., 2011), adolescents (Pugliese et al., 2009), and children (Samson et al., 2016) with ASD. The UNC, which connects the orbitofrontal cortex to the anterior temporal cortex, plays a putative role in verbal communication and social emotional processing (Von Der Heide et al., 2013). Previous studies have reported that reduced FA in the right UNC is related to antisocial behavior (Craig et al., 2009), altered verbal communication (Mabbott et al., 2009) and emotional cognition (Schmahmann et al., 2008).

We also found decreased FA and tract length in the left CCG in ASD individuals compared to TD individuals. Our findings support previous

studies demonstrating decreased FA in the left CCG in individuals with ASD (Barnea-Goraly et al., 2004; Ikuta et al., 2014; Noriuchi et al., 2010). The CCG connects the cingulate with other brain regions, and is the most prominent white matter pathway in the limbic system (Basser et al., 1994). This structure has also been associated with social interaction as measured by emotional cognition tasks (Fujiwara et al., 2007).

Tract length in the CCG refers to the distance between the medial frontal cortex and the occipital cortex (Catani and Thiebaut de Schotten, 2008). We found that decreased tract length of the left CCG to be associated with increased SCQ total scores. The SCQ was designed to focus not only on communication, but also on social interaction and restricted,

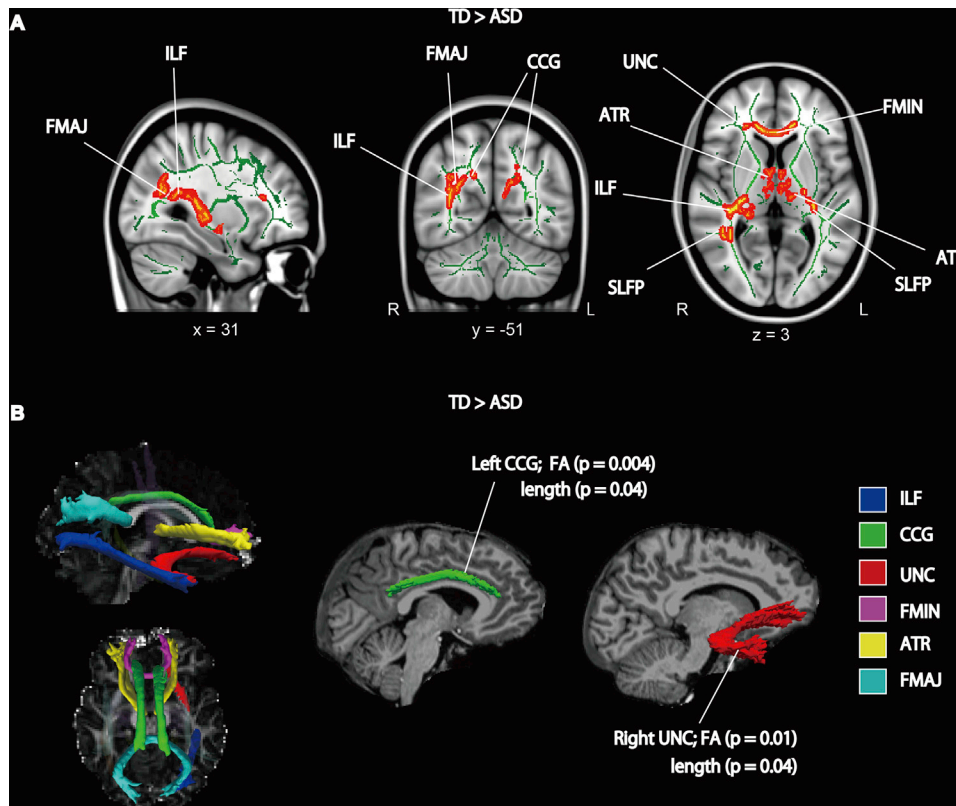


Fig. 1. A: Results of tract-based spatial statistics analysis of fractional anisotropy (FA). Differences were observed in the right inferior longitudinal fasciculus (ILF), bilateral anterior thalamic radiation (ATR), bilateral cingulum – cingulate gyrus supracallosal bundle (CCG), right uncinate fasciculus (UNC), corpus callosum – forceps major (FMAJ), and corpus callosum – forceps minor (FMIN) between individuals with autism spectrum disorder (ASD) and individuals with typical development (TD). Results were obtained with threshold-free cluster enhancement with number of permutations set at 10000 ($p < 0.05$ FWE corrected). B: Results of probabilistic reconstruction analysis. Reconstructed brain map of left CCG (green) and right UNC (red) in a study individual, using the global probabilistic algorithm proposed in TRACULA software. ASD group showed decreased FA ($p = 0.004$) and track length ($p = 0.04$) in the left CCG. ASD group also showed decreased FA ($p = 0.01$) and track length ($p = 0.04$) in the right UNC. One way analysis of covariance was performed with three regressors (site, IQ, and age) using SPSS ($p < 0.05$).

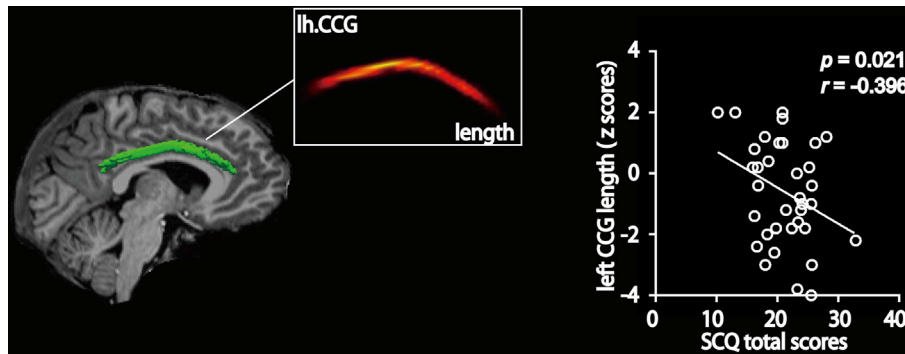


Fig. 2. Relationship between CCG and core symptom severity. Reconstructed brain map of left CCG (green) in a study individual, using the global probabilistic algorithm proposed in TRACULA software. Difference in lateral occipital cortex is correlated with ADI-R non-verbal score ($p = 0.007$; $r = -0.439$).

repetitive, and stereotyped behaviors (Chandler et al., 2007). A recent study showed a significant positive correlation between the functional activation of the CCG and the functional activation of the default mode network (DMN), a network involved in social cognition (van den Heuvel et al., 2008). Taken together, these results suggest that the hallmark of ASD, atypical social interaction and verbal-communication, may stem from decreased structural connectivity in the UNC and CCG.

Individuals with ASD had significantly decreased fALFF in the right lateral occipital cortex and cuneus cortex compared to TD individuals. This result is consistent with several recent studies which reported decreased fALFF in the right occipital cortex of ASD individuals (Di Martino et al., 2014; Itahashi et al., 2015). The occipital cortex is involved in nonverbal and verbal communication, including face perception (Aleman and Swart, 2008; Gauthier et al., 2000; Gschwind

et al., 2012; Pierce et al., 2004), mentalizing (Libero et al., 2014) and language development (Lombardo et al., 2015). A previous study indicated that ASD individuals have difficulty integrating verbal and nonverbal cues during social interactions, which we speculate may be due to the decreased activation of the lateral occipital cortex (Hubbard et al., 2012). Further, altered resting-state functional activation of the lateral occipital area is associated with abnormal local and global visual processing in ASD (Abrams et al., 2013; Keown et al., 2013). Our results may provide an explanation for the atypical communication processing in the lateral occipital cortex in individuals with ASD.

Our results demonstrate that individuals with ASD have significantly reduced gray matter surface area in the occipital cortex, including the lateral occipital cortex, cuneus cortex, and pericalcarine cortex. This result is in line with our DTI and fALFF results, further highlighting the

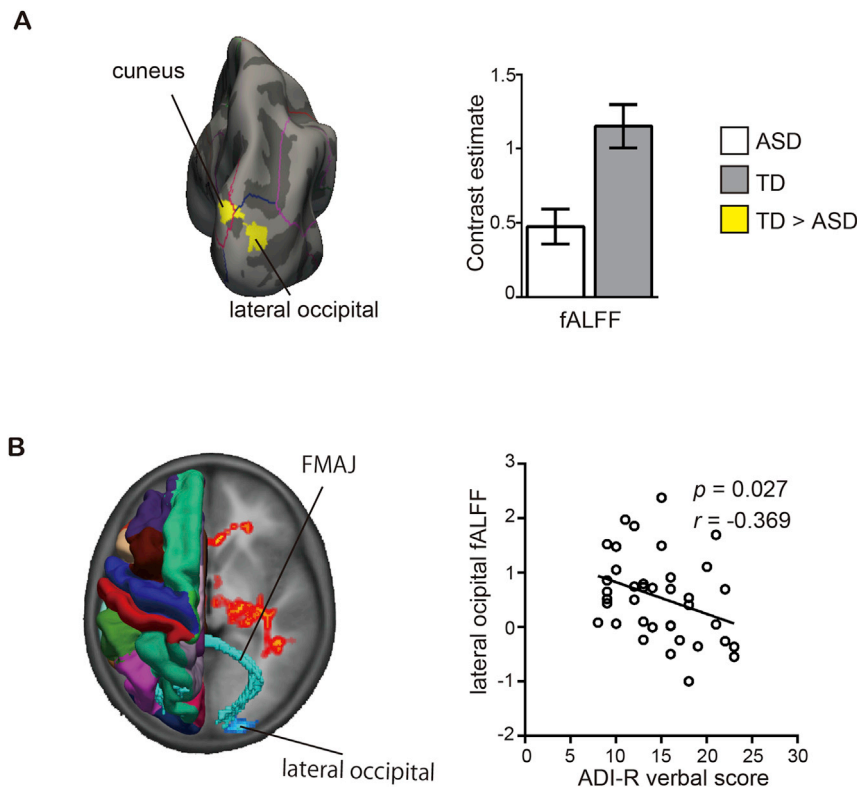


Fig. 3. A: Group differences in fractional amplitude of low-frequency fluctuations (fALFF). Yellow represents higher fALFF in the typical development (TD) group compared to the autism spectrum disorder (ASD) group in the right lateral occipital cortex and right cuneus cortex (voxel-level $Z = 2.3$; cluster significance: $P = 0.05$, gaussian random field theory corrected). Inflated brain map shows average surface area using Freesurfer. Color in brain map was calculated using parcellation in Freesurfer. Bar graph depicting fALFF contrast values at $x = 4$, $y = 100$, $z = 6$ in the lateral occipital cortex (right). B: Relationship between fALFF and core symptom severity. Brain map shows average surface area on inflated brain using parcellation by Freesurfer. Cyan shows significant group difference between ASD and TD. Cyan track shows forceps major white matter pathway. fALFF group difference in the lateral occipital cortex is correlated with ADI-R verbal score ($p = 0.027$, $r = -0.369$). Coefficient was calculated with adjustment for site, FIQ, and age using SPSS.

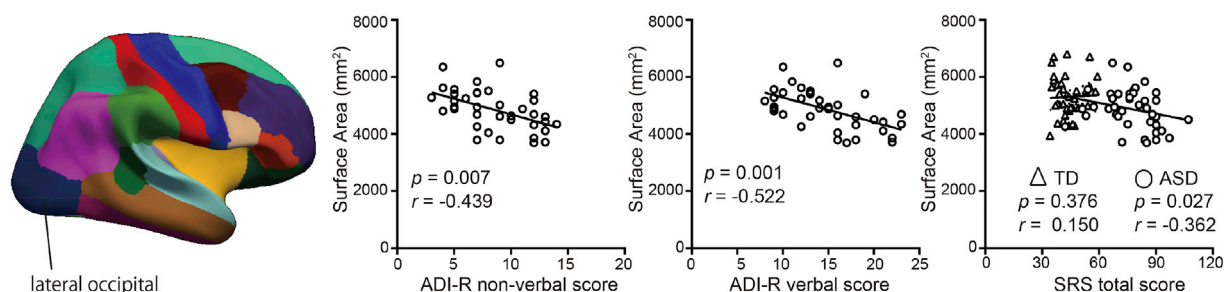


Fig. 4. Relationship between surface area and core symptom severity. Brain map shows average surface area on inflated brain using parcellation in Freesurfer. Navy indicates right lateral occipital area. Left: Surface area difference in lateral occipital cortex is correlated with ADI-R non-verbal score ($p = 0.007$; $r = -0.439$). Middle: Surface area difference in lateral occipital cortex is correlated with ADI-R verbal score ($p = 0.001$; $r = -0.522$). Right: Surface area difference in lateral occipital cortex is correlated with Total SRS score ($p = 0.027$; $r = -0.362$). Coefficients were calculated with adjustments for site, IQ, and age using SPSS.

role of the occipital cortex in ASD (Duerden et al., 2012; Nagels et al., 2015). Recent studies have demonstrated that multimodal neuroimaging may help reveal specific neurodevelopmental differences in brain structure, function, and connectivity simultaneously (Ecker et al., 2015), offering us a more comprehensive understanding of the pathology of ASD. (Ecker et al., 2015; Libero et al., 2015). In our study, fALFF and surface area measurements provided us with valuable, but different information about the role of the occipital cortex in the pathology of ASD.

We only found structural and functional changes in the right occipital cortex, which seems inconsistent with previous studies showing bilateral occipital cortex abnormalities in individuals with ASD (Di Martino et al., 2014; Wallace et al., 2013). However, at a less conservative threshold, we also found reduced fALFF ($p < 0.005$ uncorrected, cluster size 72) and surface area at the left occipital cortex (Supplementary Table 3). Our results suggest the right occipital abnormality is more predominant in ASD. Further studies are needed to validate our findings.

In this study, we included autism patients from 6 to 19 years old. Previous studies suggest that imaging abnormalities may not be static in autism through childhood and adolescence (Bos et al., 2015; Dickstein et al., 2013). In this study, there was no association between age and group differences among DTI, fALFF, and surface analysis results. A recent study (Bos et al., 2015) also did not find any interaction between group and age in surface area results in a similar age range (8–18 years). We speculate that although some imaging abnormalities are not static in autism through childhood and adolescence, others may be present in both childhood and adolescence.

There are several limitations in this study. First, we only included boys between 6 and 19 years old in our study to increase the homogeneity, therefore whether our findings can be generalized to different age and genders remains unclear. In addition, we only reported a sample size of 40 ASD individuals due to our stringent selection criteria. Future studies are needed to replicate our findings with a larger sample size.

5. Conclusions

Using a multimodal approach, we found that ASD is associated with decreased structural connectivity and resting-state brain connectivity in the occipital cortex. This disruption may impair the integration of visual communication cues in individuals with ASD, thereby impacting social communication in adolescent boys.

Funding sources

Jian Kong was supported by R01AT006364, R01AT008563, R21AT008707, R61 AT009310, and P01AT006663 from NIH/NCCIH.

Conflicts of interest

J.K. holds equity in a startup company (MNT). All other authors declare that they have no competing financial interests.

Acknowledgments

We are grateful to all the members of the Autism Brain Imaging Data Exchange Consortium (ABIDE; http://fcon_1000.projects.nitrc.org/indi/abide/) and the International Neuroimaging Data-Sharing Initiative (INDI) team (http://fcon_1000.projects.nitrc.org/) supporting the ABIDE effort (NIMH 5R21MH107045).

Appendix A. Supplementary data

Supplementary data related to this article can be found at <https://doi.org/10.1016/j.neuroimage.2017.09.031>

References

- Abrams, D.A., Lynch, C.J., Cheng, K.M., Phillips, J., Supekar, K., Ryali, S., Uddin, L.Q., Menon, V., 2013. Underconnectivity between voice-selective cortex and reward circuitry in children with autism. *Proc. Natl. Acad. Sci. U. S. A.* 110, 12060–12065. <http://dx.doi.org/10.1073/pnas.1302982110>.
- Aleman, A., Swart, M., 2008. Sex differences in neural activation to facial expressions denoting contempt and disgust. *PLoS One* 3, e3622. <http://dx.doi.org/10.1371/journal.pone.0003622>.
- Alexander, A.L., Lee, J.E., Lazar, M., Boudos, R., DuBray, M.B., Oakes, T.R., Miller, J.N., Lu, J., Jeong, E.K., McMahon, W.M., Bigler, E.D., Lainhart, J.E., 2007. Diffusion tensor imaging of the corpus callosum in Autism. *Neuroimage* 34, 61–73. <http://dx.doi.org/10.1016/j.neuroimage.2006.08.032>.
- Aoki, Y., Abe, O., Nippashi, Y., Yamasue, H., 2013. Comparison of white matter integrity between autism spectrum disorder subjects and typically developing individuals: a meta-analysis of diffusion tensor imaging tractography studies. *Mol. Autism* 4, 25. <http://dx.doi.org/10.1186/2040-2392-4-25>.
- Barnea-Goraly, N., Kwon, H., Menon, V., Eliez, S., Lotspeich, L., Reiss, A.L., 2004. White matter structure in autism: preliminary evidence from diffusion tensor imaging. *Biol. Psychiat.* 55, 323–326. <http://dx.doi.org/10.1016/j.biopsych.2003.10.022>.
- Baron-Cohen, S., Knickmeyer, R.C., Belmonte, M.K., 2005. Sex differences in the brain: implications for explaining autism. *Science* 310, 819–823. <http://dx.doi.org/10.1126/science.1115455>.
- Baron-Cohen, S., Richler, J., Bisarya, D., Guronathan, N., Wheelwright, S., 2003. The systemizing quotient: an investigation of adults with Asperger syndrome or high-functioning autism, and normal sex differences. *Philos. Trans. R. Soc. Lond. B. Biol. Sci.* 358, 361–374. <http://dx.doi.org/10.1098/rstb.2002.1206>.
- Basser, P.J., Mattiello, J., LeBihan, D., 1994. MR diffusion tensor spectroscopy and imaging. *Biophys. J.* 66, 259–267. [http://dx.doi.org/10.1016/S0006-3495\(94\)80775-1](http://dx.doi.org/10.1016/S0006-3495(94)80775-1).
- Bernard, J.A., Orr, J.M., Mittal, V.A., 2016. Differential motor and prefrontal cerebello-cortical network development: evidence from multimodal neuroimaging. *Neuroimage* 124, 591–601. <http://dx.doi.org/10.1016/j.neuroimage.2015.09.022>.
- Bos, D.J., Merchán-Naranjo, J., Martínez, K., Pina-Camacho, L., Balsa, I., Boada, L., Schnack, H., Oranje, B., Desco, M., Arango, C., Parellada, M., Durston, S., Janssen, J., 2015. Reduced gyrification is related to reduced interhemispheric connectivity in autism spectrum disorders. *J. Am. Acad. Child. Adolesc. Psychiat.* 54, 668–676. <http://dx.doi.org/10.1016/j.jaac.2015.05.011>.
- Brito, A.R., Vasconcelos, M.M., Domingues, R.C., Hygino Da Cruz, L.C., Rodrigues, L. de S., Gasparetto, E.L., Calçada, C.A.B.P., 2009. Diffusion tensor imaging findings in school-aged autistic children. *J. Neuroimaging* 19, 337–343. <http://dx.doi.org/10.1111/j.1552-6569.2009.00366.x>.
- Catani, M., Thiebaut de Schotten, M., 2008. A diffusion tensor imaging tractography atlas for virtual in vivo dissections. *Cortex* 44, 1105–1132. <http://dx.doi.org/10.1016/j.cortex.2008.05.004>.
- Chandler, S., Charman, T., Baird, G., Simonoff, E., Loucas, T., Meldrum, D., Scott, M., Pickles, A., 2007. Validation of the Social Communication Questionnaire in a population cohort of children with autism spectrum disorders. *J. Am. Acad. Child.*

- Adolesc. Psychiat. 46, 1324–1332. <http://dx.doi.org/10.1097/chi.0b013e31812f7d8d>.
- Constantino, J.N., Davis, S.A., Todd, R.D., Schindler, M.K., Gross, M.M., Brophy, S.L., Metzger, L.M., Shoushtari, C.S., Splinter, R., Reich, W., 2003. Validation of a brief quantitative measure of autistic traits: comparison of the social responsiveness scale with the Autism Diagnostic Interview-Revised. *J. Autism Dev. Disord.* 33, 427–433. <http://dx.doi.org/10.1023/A:1025014929212>.
- Craig, M.C., Catani, M., Deeley, Q., Latham, R., Daly, E., Kanaan, R., Picchioni, M., McGuire, P.K., Fahy, T., Murphy, D.G.M., 2009. Altered connections on the road to psychopathy. *Mol. Psychiat.* 14, 946–953. <http://dx.doi.org/10.1038/mp.2009.40>, 907.
- Desikan, R.S., Ségonne, F., Fischl, B., Quinn, B.T., Dickerson, B.C., Blacker, D., Buckner, R.L., Dale, A.M., Maguire, R.P., Hyman, B.T., Albert, M.S., Killiany, R.J., 2006. An automated labeling system for subdividing the human cerebral cortex on MRI scans into gyral based regions of interest. *Neuroimage* 31, 968–980. <http://dx.doi.org/10.1016/j.neuroimage.2006.01.021>.
- Di Martino, A., Yan, C.-G., Li, Q., Denio, E., Castellanos, F.X., Alaerts, K., Anderson, J.S., Assaf, M., Bookheimer, S.Y., Dapretto, M., Deen, B., Delmonte, S., Dinstein, I., Ertl-Wagner, B., Fair, D.A., Gallagher, L., Kennedy, D.P., Keown, C.L., Keyser, C., Lainhart, J.E., Lord, C., Luna, B., Menon, V., Minshew, N.J., Monk, C.S., Mueller, S., Müller, R., Nebel, M.B., Nigg, J.T., O’Hearn, K., Pelphey, K.A., Peltier, S.J., Rudie, J.D., Sunaert, S., Thieux, M., Tyszka, J.M., Uddin, L.Q., Verhoeven, J.S., Wenderoth, N., Wiggins, J.L., Mostofsky, S.H., Milham, M.P., 2014. The autism brain imaging data exchange: towards a large-scale evaluation of the intrinsic brain architecture in autism. *Mol. Psychiat.* 19, 659–667. <http://dx.doi.org/10.1038/mp.2013.78>.
- Di Martino, A., Zuo, X.-N., Kelly, C., Grzadzinski, R., Mennes, M., Schvarcz, A., Rodman, J., Lord, C., Castellanos, F.X., Milham, M.P., 2013. Shared and distinct intrinsic functional network centrality in autism and attention-deficit/hyperactivity disorder. *Biol. Psychiat.* 74, 623–632. <http://dx.doi.org/10.1016/j.biopsych.2013.02.011>.
- Dichter, G.S., Belger, A., 2007. Social stimuli interfere with cognitive control in autism. *Neuroimage* 35, 1219–1230. <http://dx.doi.org/10.1016/j.neuroimage.2006.12.038>.
- Dickstein, D.P., Pescosolido, M.F., Reidy, B.L., Galvan, T., Kim, K.L., Seymour, K.E., Laird, A.R., Di Martino, A., Barrett, R.P., 2013. Developmental meta-analysis of the functional neural correlates of autism spectrum disorders. *J. Am. Acad. Child. Adolesc. Psychiat.* 52, 279–289. <http://dx.doi.org/10.1016/j.jaac.2012.12.012> e16.
- Duerden, E.G., Mak-Fan, K.M., Taylor, M.J., Roberts, S.W., 2012. Regional differences in grey and white matter in children and adults with autism spectrum disorders: an activation likelihood estimate (ALE) meta-analysis. *Autism Res.* 5, 49–66. <http://dx.doi.org/10.1002/aur.235>.
- Ecker, C., Bookheimer, S.Y., Murphy, D.G.M., 2015. Neuroimaging in autism spectrum disorder: brain structure and function across the lifespan. *Lancet Neurol.* 14, 1121–1134. [http://dx.doi.org/10.1016/S1474-4422\(15\)00050-2](http://dx.doi.org/10.1016/S1474-4422(15)00050-2).
- Fischl, B., 2012. Free. *Neuroimage*. <http://dx.doi.org/10.1016/j.neuroimage.2012.01.021>.
- Fischl, B., Sereno, M.I., Dale, A.M., 1999a. Cortical surface-based analysis: II: inflation, flattening, and a surface-based coordinate system. *Neuroimage* 9, 195–207. <http://dx.doi.org/10.1006/nimg.1998.0396>.
- Fischl, B., Sereno, M.I., Tootell, R.B.H., Dale, A.M., 1999b. High-resolution intersubject averaging and a coordinate system for the cortical surface. *Hum. Brain Mapp.* 8, 272–284. [http://dx.doi.org/10.1002/\(SICI\)1097-0193\(1999\)8:4<272::AID-HBM10>3.0.CO;2-4](http://dx.doi.org/10.1002/(SICI)1097-0193(1999)8:4<272::AID-HBM10>3.0.CO;2-4).
- Fischl, B., Van Der Kouwe, A., Destrieux, C., Halgren, E., Ségonne, F., Salat, D.H., Busa, E., Seidman, L.J., Goldstein, J., Kennedy, D., Caviness, V., Makris, N., Rosen, B., Dale, A.M., 2004. Automatically parcellating the human cerebral cortex. *Cereb. Cortex* 14, 11–22. <http://dx.doi.org/10.1093/cercor/bhg087>.
- Friedman, L., Stern, H., Brown, G.G., Mathalon, D.H., Turner, J., Glover, G.H., Gollub, R.L., Lauriello, J., Lim, K.O., Cannon, T., Greve, D.N., Bockholt, H.J., Belger, A., Mueller, B., Doty, M.J., He, J., Wells, W., Smyth, P., Pieper, S., Kim, S., Kubicki, M., Vangel, M., Potkin, S.G., 2008. Test-retest and between-site reliability in a multicenter fMRI study. *Hum. Brain Mapp.* 29, 958–972. <http://dx.doi.org/10.1002/hbm.20440>.
- Fujiwara, H., Hirao, K., Namiki, C., Yamada, M., Shimizu, M., Fukuyama, H., Hayashi, T., Murai, T., 2007. Anterior cingulate pathology and social cognition in schizophrenia: a study of gray matter, white matter and sulcal morphometry. *Neuroimage* 36, 1236–1245. <http://dx.doi.org/10.1016/j.neuroimage.2007.03.068>.
- Gauthier, I., Skudlarski, P., Gore, J.C., Anderson, A.W., 2000. Expertise for cars and birds recruits brain areas involved in face recognition. *Nat. Neurosci.* 3, 191–197. <http://dx.doi.org/10.1038/72140>.
- Gschwind, M., Pourtois, G., Schwartz, S., Van De Ville, D., Vuilleumier, P., 2012. White-matter connectivity between face-responsive regions in the human brain. *Cereb. Cortex* 22, 1564–1576. <http://dx.doi.org/10.1093/cercor/bhr226>.
- Han, X., Jovicich, J., Salat, D., van der Kouwe, A., Quinn, B., Czanner, S., Busa, E., Pacheco, J., Albert, M., Killiany, R., Maguire, P., Rosas, D., Makris, N., Dale, A., Dickerson, B., Fischl, B., 2006. Reliability of MRI-derived measurements of human cerebral cortical thickness: the effects of field strength, scanner upgrade and manufacturer. *Neuroimage* 32, 180–194. <http://dx.doi.org/10.1016/j.neuroimage.2006.02.051>.
- Hubbard, A.L., McNealy, K., Scott-Van Zeeland, A.A., Callan, D.E., Bookheimer, S.Y., Dapretto, M., 2012. Neuropsychopharmacology. *Brain Behav.* 2, 606–619. <http://dx.doi.org/10.1002/brb3.81>.
- Ikuta, T., Shafritz, K.M., Bregman, J., Peters, B.D., Gruner, P., Malhotra, A.K., Szeszkó, P.R., 2014. Abnormal cingulum bundle development in autism: a probabilistic tractography study. *Psychiatry Res. Neuroimaging* 221, 63–68. <http://dx.doi.org/10.1016/j.psychres.2013.08.002>.
- Itahashi, T., Yamada, T., Watanabe, H., Nakamura, M., Ohta, H., Kanai, C., Iwanami, A., Kato, N., Hashimoto, R., 2015. Alterations of local spontaneous brain activity and connectivity in adults with high-functioning autism spectrum disorder. *Mol. Autism* 6, 1–14. <http://dx.doi.org/10.1186/s13229-015-0026-z>.
- Jung, M., Kosaka, H., Saito, D.N., Ishitobi, M., Morita, T., Inohara, K., Asano, M., Arai, S., Munese, T., Tomoda, A., Wada, Y., Sadato, N., Okazawa, H., Iidaka, T., 2014. Default mode network in young male adults with autism spectrum disorder: relationship with autism spectrum traits. *Mol. Autism* 5, 35. <http://dx.doi.org/10.1186/2040-2392-5-35>.
- Keown, C., Shih, P., Nair, A., Peterson, N., Mulvey, M., Müller, R.A., 2013. Local functional overconnectivity in posterior brain regions is associated with symptom severity in autism spectrum disorders. *Cell Rep.* 5, 567–572. <http://dx.doi.org/10.1016/j.celrep.2013.10.003>.
- Kumar, A., Sundaram, S.K., Sivaswamy, L., Behen, M.E., Makki, M.I., Ager, J., Janisse, J., Chugani, H.T., Chugani, D.C., 2010. Alterations in frontal lobe tracts and corpus callosum in young children with autism spectrum disorder. *Cereb. Cortex* 20, 2103–2113. <http://dx.doi.org/10.1093/cercor/bhp278>.
- Lai, M.-C., Lombardo, M.V., Baron-Cohen, S., 2014. Autism. *Lancet* 383, 896–910. [http://dx.doi.org/10.1016/S0140-6736\(13\)61539-1](http://dx.doi.org/10.1016/S0140-6736(13)61539-1).
- Libero, L.E., DeRamus, T.P., Lahti, A.C., Deshpande, G., Kana, R.K., 2015. Multimodal neuroimaging based classification of autism spectrum disorder using anatomical, neurochemical, and white matter correlates. *Cortex* 66, 46–59. <http://dx.doi.org/10.1016/j.cortex.2015.02.008>.
- Libero, L.E., Maximo, J.O., Deshpande, H.D., Klinger, L.G., Klinger, M.R., Kana, R.K., 2014. The role of mirroring and mentalizing networks in mediating action intentions in autism. *Mol. Autism* 5, 50. <http://dx.doi.org/10.1186/2040-2392-5-50>.
- Lombardo, M.V., Pierce, K., Eyer, L.T., Carter Barnes, C., Ahrens-Barbeau, C., Solso, S., Campbell, K., Courchesne, E., 2015. Different functional neural substrates for good and poor language outcome in autism. *Neuron* 1–11. <http://dx.doi.org/10.1016/j.neuron.2015.03.023>.
- Lord, C., Risi, S., Lambrecht, L., Cook Jr., E.H., Leventhal, B.L., DiLavore, P.C., Pickles, A., Rutter, M., 2000. The Autism Diagnostic Observation Schedule—generic: A standard measure of social and communication deficits associated with the spectrum of autism. *J. Autism Dev. Disord.* 30, 205–223.
- Lord, C., Rutter, M., Le Couteur, A., 1994. Autism Diagnostic Interview-Revised: a revised version of a diagnostic interview for caregivers of individuals with possible pervasive developmental disorders. *J. Autism Dev. Disord.* 24, 659–685.
- Mabbott, D.J., Rovet, J., Noseworthy, M.D., Smith, M.Lou, Rockel, C., 2009. The relations between white matter and declarative memory in older children and adolescents. *Brain Res.* 1294, 80–90. <http://dx.doi.org/10.1016/j.brainres.2009.07.046>.
- Mazaika, P.K., Hoeft, F., Glover, G.H., Reiss, A.L., 2009. Methods and software for fMRI analysis of clinical subjects. *Neuroimage* 47, S58. [http://dx.doi.org/10.1016/S1053-8119\(09\)70238-1](http://dx.doi.org/10.1016/S1053-8119(09)70238-1).
- Muschelli, J., Nebel, M.B., Caffo, B.S., Barber, A.D., Pekar, J.J., Mostofsky, S.H., 2014. Reduction of motion-related artifacts in resting state fMRI using aCompCor. *Neuroimage* 96, 22–35. <http://dx.doi.org/10.1016/j.neuroimage.2014.03.028>.
- Myers, C.A., Wang, C., Black, J.M., Bugescu, N., Hoeff, F., 2016. The matter of motivation: striatal resting-state connectivity is dissociable between grit and growth mindset. *Soc. Cogn. Affect. Neurosci.* 11, 1521–1527. <http://dx.doi.org/10.1093/scan/nsw065>.
- Nagels, A., Kircher, T., Steins, M., Straube, B., 2015. Feeling addressed! the role of body orientation and co-speech gesture in social communication. *Hum. Brain Mapp.* 36, 1925–1936. <http://dx.doi.org/10.1002/hbm.22746>.
- Noriuchi, M., Kikuchi, Y., Yoshiura, T., Kira, R., Shigetoh, H., Hara, T., Tobimatsu, S., Kamio, Y., 2010. Altered white matter fractional anisotropy and social impairment in children with autism spectrum disorder. *Brain Res.* 1362, 141–149. <http://dx.doi.org/10.1016/j.brainres.2010.09.051>.
- Pierce, K., Haist, F., Sedaghat, F., Courchesne, E., 2004. The brain response to personally familiar faces in autism: findings of fusiform activity and beyond. *Brain* 127, 2703–2716. <http://dx.doi.org/10.1093/brain/awh289>.
- Pugliese, L., Catani, M., Ameis, S., Dell’Acqua, F., de Schotten, M.T., Murphy, C., Robertson, D., Deeley, Q., Daly, E., Murphy, D.G.M., 2009. The anatomy of extended limbic pathways in Asperger syndrome: a preliminary diffusion tensor imaging tractography study. *Neuroimage* 47, 427–434. <http://dx.doi.org/10.1016/j.neuroimage.2009.05.014>.
- Redcay, E., Moran, J.M., Mavros, P.L., Tager-Flusberg, H., Gabrieli, J.D.E., Whitfield-Gabrieli, S., 2013. Intrinsic functional network organization in high-functioning adolescents with autism spectrum disorder. *Front. Hum. Neurosci.* 7, 573. <http://dx.doi.org/10.3389/fnhum.2013.00573>.
- Samson, A.C., Dougherty, R.F., Lee, I.A., Phillips, J.M., Gross, J.J., Hardan, A.Y., 2016. White matter structure in the uncinate fasciculus: implications for socio-affective deficits in Autism Spectrum Disorder. *Psychiat. Res. Neuroimaging* 255, 66–74. <http://dx.doi.org/10.1016/j.psychres.2016.08.004>.
- Schaer, M., Ottet, M.-C., Scariati, E., Dukes, D., Franchini, M., Eliez, S., Glaser, B., 2013. Decreased frontal gyrification correlates with altered connectivity in children with autism. *Front. Hum. Neurosci.* 7, 750. <http://dx.doi.org/10.3389/fnhum.2013.00750>.
- Schmahmann, J.D., Smith, E.E., Eichler, F.S., Filley, C.M., 2008. Cerebral white matter: neuroanatomy, clinical neurology, and neurobehavioral correlates. *Ann. N. Y. Acad. Sci.* <http://dx.doi.org/10.1196/annals.1444.017>.
- Smith, S.M., Jenkinson, M., Johansen-Berg, H., Rueckert, D., Nichols, T.E., Mackay, C.E., Watkins, K.E., Ciccarelli, O., Cader, M.Z., Matthews, P.M., Behrens, T.E.J., 2006. Tract-based spatial statistics: voxelwise analysis of multi-subject diffusion data. *Neuroimage* 31, 1487–1505. <http://dx.doi.org/10.1016/j.neuroimage.2006.02.024>.
- Smith, S.M., Jenkinson, M., Woolrich, M.W., Beckmann, C.F., Behrens, T.E.J., Johansen-Berg, H., Bannister, P.R., De Luca, M., Drobnjak, I., Flitney, D.E., Niazy, R.K., Saunders, J., Vickers, J., Zhang, Y., De Stefano, N., Brady, J.M., Matthews, P.M.,

2004. Advances in functional and structural MR image analysis and implementation as FSL. *NeuroImage* S208–S219. <http://dx.doi.org/10.1016/j.neuroimage.2004.07.051>.
- Smith, S.M., Nichols, T.E., 2009. Threshold-free cluster enhancement: addressing problems of smoothing, threshold dependence and localisation in cluster inference. *Neuroimage* 44, 83–98. <http://dx.doi.org/10.1016/j.neuroimage.2008.03.061>.
- Thomas, C., Humphreys, K., Jung, K.J., Minshew, N., Behrmann, M., 2011. The anatomy of the callosal and visual-association pathways in high-functioning autism: a DTI tractography study. *Cortex* 47, 863–873. <http://dx.doi.org/10.1016/j.cortex.2010.07.006>.
- Travers, B.G., Adluru, N., Ennis, C., Tromp, D.P.M., Destiche, D., Doran, S., Bigler, E.D., Lange, N., Lainhart, J.E., Alexander, A.L., 2012. Diffusion tensor imaging in autism spectrum disorder: a review. *Autism Res.* <http://dx.doi.org/10.1002/aur.1243>.
- Uddin, L.Q., Supekar, K., Lynch, C.J., Khouzam, A., Phillips, J., Feinstein, C., Ryali, S., Menon, V., 2013. Salience network-based classification and prediction of symptom severity in children with autism. *JAMA Psychiat.* 70, 869–879. <http://dx.doi.org/10.1001/jamapsychiatry.2013.104>.
- van den Heuvel, M., Mandl, R., Luigjes, J., Hulshoff Pol, H., 2008. Microstructural organization of the cingulum tract and the level of default mode functional connectivity. *J. Neurosci.* 28, 10844–10851. <http://dx.doi.org/10.1523/JNEUROSCI.2964-08.2008>.
- von dem Hagen, E.A.H., Stoyanova, R.S., Baron-Cohen, S., Calder, A.J., 2013. Reduced functional connectivity within and between “social” resting state networks in autism spectrum conditions. *Soc. Cogn. Affect. Neurosci.* 8, 694–701. <http://dx.doi.org/10.1093/Scan/Nss053>.
- Von Der Heide, R.J., Skipper, L.M., Klobusicky, E., Olson, I.R., 2013. Dissecting the uncinate fasciculus: disorders, controversies and a hypothesis. *Brain.* <http://dx.doi.org/10.1093/brain/awt094>.
- Walker, L., Gozzi, M., Lenroot, R., Thurm, A., Behseta, B., Swedo, S., Pierpaoli, C., 2012. Diffusion tensor imaging in young children with autism: biological effects and potential confounds. *Biol. Psychiat.* 72, 1043–1051. <http://dx.doi.org/10.1016/j.biopsych.2012.08.001>.
- Wallace, G.L., Robustelli, B., Dankner, N., Kenworthy, L., Giedd, J.N., Martin, A., 2013. Increased gyrification, but comparable surface area in adolescents with autism spectrum disorders. *Brain* 136, 1956–1967. <http://dx.doi.org/10.1093/brain/awt106>.
- Wang, X., Wang, Z., Liu, J., Chen, J., Liu, X., Nie, G., Byun, J.S., Liang, Y., Park, J., Huang, R., Liu, M., Liu, B., Kong, J., 2016. Repeated acupuncture treatments modulate amygdala resting state functional connectivity of depressive patients. *NeuroImage Clin.* 12, 746–752. <http://dx.doi.org/10.1016/j.nicl.2016.07.011>.
- White, T., Magnotta, V.A., Bockholt, H.J., Williams, S., Wallace, S., Ehrlich, S., Mueller, B.A., Ho, B.C., Jung, R.E., Clark, V.P., Laurillo, J., Bustillo, J.R., Schulz, S.C., Gollub, R.L., Andreasen, N.C., Calhoun, V.D., Lim, K.O., 2011. Global white matter abnormalities in schizophrenia: a multisite diffusion tensor imaging study. *Schizophr. Bull.* 37, 222–232. <http://dx.doi.org/10.1093/schbul/sbp088>.
- Whitfield-Gabrieli, S., Nieto-Castanon, A., 2012. CONN: a functional connectivity toolbox for correlated and anticorrelated brain networks. *Brain Connect.* 2, 125–141. <http://dx.doi.org/10.1089/brain.2012.0073>.
- Yendiki, A., Koldewyn, K., Kakunoori, S., Kanwisher, N., Fischl, B., 2014. Spurious group differences due to head motion in a diffusion MRI study. *Neuroimage* 88, 79–90. <http://dx.doi.org/10.1016/j.neuroimage.2013.11.027>.
- Yendiki, A., Panneck, P., Srinivasan, P., Stevens, A., Zöllei, L., Augustinack, J., Wang, R., Salat, D., Ehrlich, S., Behrens, T., Jbabdi, S., Gollub, R., Fischl, B., 2011. Automated probabilistic reconstruction of white-matter pathways in health and disease using an atlas of the underlying anatomy. *Front. Neuroinform* 5, 23. <http://dx.doi.org/10.3389/fninf.2011.00023>.